Improving Calibration and Validation of Cosmic-Ray Neutron Sensors in the Light of Spatial Sensitivity – Theory and Evidence

Martin Schrön[1,2], Markus Köhli[1,3,4], Lena Scheiffele[5], Joost Iwema[6], Heye R. Bogena[7], Ling Lv[8], Edoardo Martini[1], Gabriele Baroni[2,5], Rafael Rosolem[6,9], Jannis Weimar[3], Juliane Mai[2,10], Matthias Cuntz[2,11], Corinna Rebmann[2], Sascha E. Oswald[5], Peter Dietrich[1], Ulrich Schmidt[3], and Steffen Zacharias[1]

[1]Dep. Monitoring and Exploration Technologies, Helmholtz Centre for Environmental Research - UFZ Leipzig, Germany
[2]Dep. Computational Hydrosystems, Helmholtz Centre for Environmental Research - UFZ Leipzig, Germany
[3]Physikalisches Institut, Heidelberg University
[4]Physikalisches Institut, University of Bonn, Germany
[5]Institute of Earth and Environmental Science, University of Potsdam, Germany
[6]Faculty of Engineering, University of Bristol, England
[7]Agrosphere Institute (IBG-3), Forschungszentrum Jülich GmbH, Germany
[8]Department of Plants, Soils and Climate, Utah State University, US
[9]Cabot Institute, University of Bristol, England
[10]Department of Civil and Environmental Engineering, University of Waterloo, Canada
[11]INRA, Université de Lorraine, UMR1137 Ecology et Ecophysiologie Forestière, Champenoux, France

Correspondence to: Martin Schrön (martin.schroen@ufz.de)

Abstract. In the last years the method of cosmic-ray neutron sensing (CRNS) has gained popularity among soil hydrologists, physicists, and land-surface modelers. The sensor provides continuous soil moisture data, averaged over several hectares and tens of decimeters depth. However, the signal still may contain unidentified features of hydrological processes, and many calibration datasets are often required in order to find reliable relations between neutrons and water dynamics. Recent insights into environmental neutrons accurately described the spatial sensitivity of the sensor and thus allowed to quantify the contribution of individual sample locations to the CRNS signal. Consequently, data points of calibration and validation datasets are suggested to be averaged using a more physically-based weighting approach. In this work, a revised sensitivity function is used to calculate weighted averages of point data. The approach is extensively tested with two calibration and four time series datasets from a variety of sites and conditions. In all cases, the revised averaging method robustly improved the performance of the CRNS product and even helped to reveal otherwise hidden hydrological processes. The presented approach increases the overall accuracy of CRNS products and will have impact on all their applications in agriculture, hydrology, and modeling.

1 Introduction

Field-scale soil moisture is an important variable to drive and evaluate agricultural, hydrological, and land-surface models (Vereecken et al., 2008; Robinson et al., 2008). Knowledge about soil moisture states at relevant scales would have direct implications for flood risk assessment (Norbiato et al., 2008), real-time estimation of water deficit in agriculture (Smith et al.,

2002), or drought forecasting and analysis (Sheffield, 2004; Samaniego et al., 2013; Ceppi et al., 2014; Zink et al., 2016). Consequently, there is a huge demand for accurate estimations of root-zone soil moisture at scales from 10 to 10^4 m.

Cosmic-ray neutron sensors (CRNS) are one of the most promising technologies for root-zone soil moisture monitoring at the field scale. These instruments are able to continuously measure soil water content averaged over several hectares and up to

5 half a meter depth (Zreda et al., 2012; Köhli et al., 2015). They are one of the few candidates to close the inconvenient scale gap between point data and remote-sensing products (Robinson et al., 2008; Bogena et al., 2015).

After the measurement method was first presented by Zreda et al. (2008), many studies were dedicated to calibrate the sensors and to assess the performance in comparison to conventional instruments (e.g., Rivera Villarreyes et al., 2011; Franz et al., 2012a; Coopersmith et al., 2014; Hawdon et al., 2014; Almeida et al., 2014). These studies showed a good agreement

10 between neutron intensity and independent soil moisture observations. However, outstanding features were also reported in the CRNS data which did not fit well to the accepted theory described by Desilets et al. (2010). Authors suggested that additional hydrological processes and hydrogen pools could influence the signal (e.g. Franz et al., 2013a; Baatz et al., 2014; Baroni and Oswald, 2015), while others applied recalibration of semi-physical parameters to better fit individual site conditions (e.g., Rivera Villarreyes et al., 2011; Lv et al., 2014; Iwema et al., 2015; Heidbüchel et al., 2016). Despite the unambiguous

15 improvements obtained by corrections and realibration approaches, still some features in many datasets could not be explained by the given theory and consequently seemed to be unrelated to hydrological processes.

To address some of these knowledge gaps, Franz et al. (2012b) investigated soil hydrological processes with water transport simulations and found that wetting and drying cycles are non-uniquely represented by the CRNS signal. Due to the integrative neutron signal, those hysteresis effects can be most significant when sharp wetting or drying fronts are shaping the soil water

20 profile. As a consequence, Franz et al. (2012b) and Franz et al. (2013b) recommended vertical weighting of point measurements in the profile to account for these effects. Furthermore, Franz et al. (2013b) also demonstrated that the sensor could underestimate average soil moisture by up to $10\,\%_{vol}$ depending on the horizontal distribution of water content in the footprint. They concluded that exact knowledge of the heterogeneity is a prerequisite for the interpretation of neutron count rates, and distance-weighting procedures are necessary to obtain sufficient performance during calibration and validation with point

25 data. In order to average calibration and validation data horizontally, Franz et al. (2012a) adopted a sampling scheme based on initial calculations by Zreda et al. (2008) to give every sample an equal weight. The resulting sensor locations at 25, 75, and 200 m correspond to an almost exponential horizontal weighting function. Bogena et al. (2013) were the first who applied this horizontal weighting to an irregularly distributed point sensor network, albeit indirectly by fitting the cumulative variant. Nevertheless, many researchers still avoid horizontal weighting by virtually re-locating their irregularly distributed point sen-

30 sors to the nearest radius of 25, 75, or 200 m in post-processing mode (e.g., Franz et al., 2012a). In complex terrain, only few calibration or validation locations are accessible and their individual contribution to the neutron signal has been unknown for a long time.

As the understanding of cosmic-ray neutron physics in the environment has been more and more elaborated, Köhli et al. (2015) developed a dedicated computer model URANOS, which helped to understand the spatial sensitivity of the neutron

35 sensor. These authors revealed that the sensor is extraordinarily sensitive to the nearest few meters, rather than following a

simple exponential decrease of sensitivity as was reported by Zreda et al. (2008) and Desilets and Zreda (2013). This revision has since changed the way how CRNS measurements are interpreted. Their findings extensively describe the footprint volume in which soil water content is measured, and can now be used to develop new weighting approaches and to revisit previous data analysis.

5 Heidbüchel et al. (2016) were the first to test the impact of the revised spatial sensitivity function on the performance of their calibration data. Encouraged by their promising results, the present study has hypothesized that this new theory could enable an improved performance of CRNS calibration and validation campaigns for a huge variety of sites and conditions. We further hypothesize that the initially published relation between neutrons and water equivalent (Desilets et al., 2010) might be widely applicable without the need to calibrate all of its parameters on site-specific conditions. Eventually, an over-all improvement of

10 the CRNS data could help to identify hydrological effects more accurately (such as precipitation, ponding, evapotranspiration, and infiltration proccesses).

The paper is structured as follows: Firstly, we present the *equally weighted*, the *conventional*, and the *revised* formulation of the spatial sensitivity function (also called *weighting function*). We then provide a procedure to generate a weighted average of point measurements that can be compared with the CRNS product. The assumptions and uncertainties of this approach are

15 then discussed, followed by a short description of measures used to evaluate the calibration and validation performance, and short descriptions of the studied sites. In the results section we present and discuss the sensor performance using the *equal*, *conventional* and the *revised* weighting approaches for calibration campaigns at two different sites, and for time series data at four sites.

2 Methods

20 Stationary cosmic-ray neutron sensors (CRNS) are particle detectors that monitor the well-mixed neutron intensity in the air (Zreda et al., 2012). Due to the low interaction probability of neutrons with air molecules, the measured particles can travel distances of up to $240\,\mathrm{m}$ from the soil to the detector (Köhli et al., 2015). The neutron signal is predominantly sensitive to the number of hydrogen atoms in the footprint, but it is also influenced by changes of air pressure, air humidity, and incoming cosmic radiation. These additional factors can be excluded by standard correction approaches (Hawdon et al., 2014; Schrön

25 et al., 2015), such that the remaining signal only represents the hydrogen abundance in the soil and biosphere. To convert the neutron count rate N to gravimetric soil water equivalent, θ, Desilets et al. (2010) suggested the following theoretical relation:

$$\theta(N) = \frac{0.0808}{N/N_0 - 0.372} - 0.115 \,, \quad \text{(Desilets et al. 2010)} \tag{1}$$

where N_0 is a site-specific calibration parameter. It is determined once for each dataset by comparing the CRNS product, $\theta(N)$, with the actual soil moisture condition in the field. However, neutrons are sensitive to all kinds of hydrogen in the footprint,

30 hence the variable θ denotes not only soil moisture, θ_{sm}, but is rather assumed to also include lattice water, θ_{lw}, as well as water equivalent from soil organic carbon, θ_{org}, and biomass, θ_{bio}:

$$\theta = \theta_{\mathrm{sm}} + \theta_{\mathrm{lw}} + \theta_{\mathrm{org}} + \theta_{\mathrm{bio}}.$$

For calibration and validation purposes, the water equivalent in the footprint volume is typically determined independently by an average of point measurements, for example from gravimetric samples or data from soil moisture monitoring networks. However, those locations can contribute differently to the apparent average of soil moisture as seen by the neutron detector,

5 for example, depending on their distance r from the CRNS probe and their depth d below the soil surface. Depending on their individual contributions, different weights can be assigned to each data point in the calculation of a so-called weighted average.

Among the variety of weighting concepts in the literature, we have selected two of the main and most frequently used strategies from recognized publications, which are based on distinct physical assumptions. On the one hand, the *conventional* approach covers the main strategies applied so far (Franz et al., 2012b; Bogena et al., 2013). On the other hand, a *revised*

10 weighting approach has been used which is based on recent findings from Köhli et al. (2015) and which has been further advanced in the present work by the following points:

- extension of the analytical fit of the radial sensitivity function W_r to low distances, $r \leq 0.5\,\mathrm{m}$,

- added dependency of the weighting functions on air pressure p and vegetation height H_{veg}, by introducing a rescaled distance $r^*(r, p, H_{\mathrm{veg}}, \theta)$.

15 The neutron transport model `URANOS` has been updated accordingly to provide advanced analytical functions for the spatial sensitivity (`URANOS 0.97`, available from www.ufz.de/uranos). These advancements generalize the applicability of the results from Köhli et al. (2015) and are recommended for future applications. Please refer to Appendix A for detailed explanations. There are certainly more factors that influence the shape of the neutron sensitivity, for example the height of the detector above ground, different plant species, and large objects. However, those factors are of minor importance for the conclusions in

20 this manuscript and should be investigated in future studies.

In addition to the *conventional* and the *revised* approach, this work includes the *equal average* weighting strategy (weights equal 1) to compare the performance when the CRNS signal is intuitively treated as a large-area averaging soil moisture product, as was done especially at macroscopically homogeneous sites.

2.1 Vertical weighting in the soil profile

25 Simulations by Zreda et al. (2008), Franz et al. (2012b), and Köhli et al. (2015) have shown that the neutron signal integrated over a vertical soil column exhibits the highest sensitivity to the uppermost layers. Therefore, independent soil moisture measurements taken at different depths, d, need to be weighted differently in order to account for the underlying physical processes. To show the consequences of neglecting this step in post-processing, we have compared the *equal* average of soil samples with alternative weighting approaches.
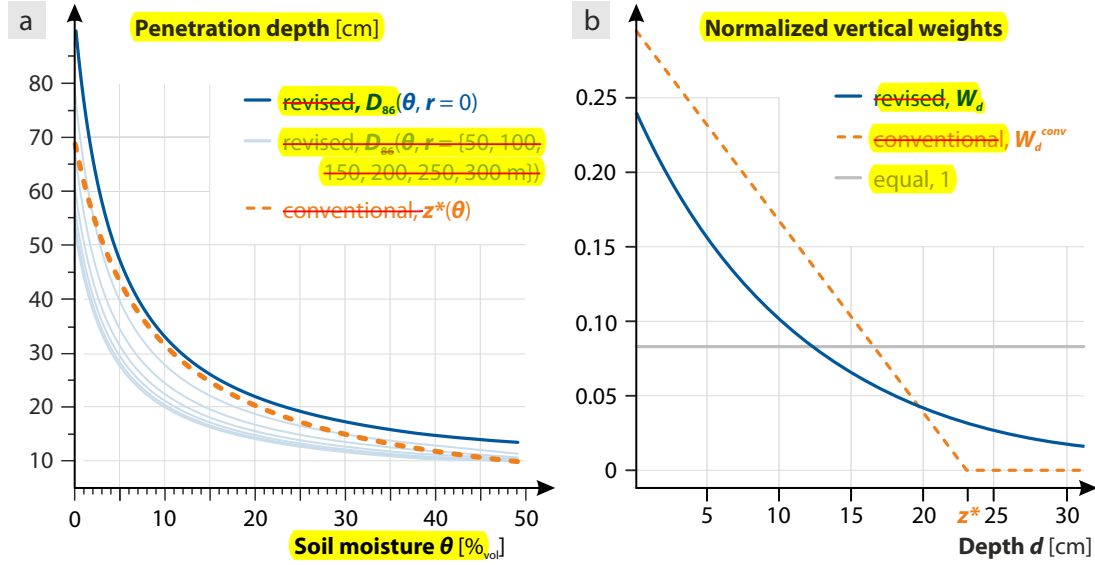
Figure 1. (a) A comparison between the *revised* and the *conventional* penetration depths, $D_{86}(\theta, r, \varrho_{\mathrm{bulk}} = 1.4\,\mathrm{g/m}^3)$ and $z^*(\theta)$, respectively. On average, both approaches follow an almost similar shape, however the conventional formulation is independent of distance r and soil bulk density ϱ_{bulk}. (b) Normalized vertical weighting functions (eqs. 2 and 3) show that the conventional approach underestimates the relative contribution from shallow water and neglects contributions from depths beyond z^* ($= 23\,\mathrm{cm}$ in this example).

The *conventional* vertical weighting, W_d^{conv}, is performed using a linear relation from Franz et al. (2012b), which was based on Monte-Carlo simulations from Zreda et al. (2008) and became widely accepted in most previous studies.

$$
W_d^{\mathrm{conv}} = \begin{cases} 1 - d/z^*, & d \le z^* \\ 0, & d > z^* \end{cases}
$$
(2)

penetration depth: $\quad z^*(\theta) = \dfrac{5.8}{\theta + 0.0829}, \quad$ in cm.

The two major shortcomings of this function are (1) that it assumes similar penetration depths of detected neutrons for all distances r from the sensor (see Fig. 1a), and (2) that it neglects any contribution of soil water below a certain cutoff depth z^* (see Fig. 1b).

In contrast, the *revised* vertical weighting function, W_d, takes the full soil profile into account (as neutrons do) and considers the fact that the effective depth decreases with increasing distance r from the detector:

$$
W_d(r, \theta, p, H_{\mathrm{veg}}) = e^{-2d/D_{86}},
$$
(3)

penetration depth: $\quad D_{86} = D_{86}(r^*, \theta, \varrho_{\mathrm{bulk}}), \quad$ in cm, see Appendix A.

where D_{86} denotes the effective penetration depth, defined as the depth within which 86 % of neutrons probed the soil (see Köhli et al., 2015). These relations are based on URANOS simulations and follow recent insights about the physics of neutron

transport and detection near the soil-atmosphere interface. Based on the formulation from Köhli et al. (2015) the advancements of the *revised* penetration depth D_{86} now add the dependency on air pressure and vegetation height, expressed in the scaled distance term, r^*, (see Appendix A).

2.2 Horizontal weighting in the footprint area

5   In this work we make use of three horizontal weighting functions to average soil moisture measurements at distances r from the CRNS probe. First, the *equal* average (weights equal 1), which was usually applied for validation with soil moisture networks and remote sensing products. It was also used for calibration datasets if locations were arranged according to the *COSMOS standard sampling scheme*, $(25\,\text{m}, 75\,\text{m}, 200\,\text{m})$, such that the samples automatically represent areas of equal contribution to the neutron signal. These calculations were based on a simple exponential sensitivity function (Zreda et al., 2008) and presented

10   by Franz et al. (2012a) and Zreda et al. (2012).

   Second, the *conventional* weighting approach uses an (almost) exponential sensitivity function based on Monte-Carlo simulations from Zreda et al. (2008). It is implicitly referred to when using the *COSMOS standard sampling scheme* (Zreda et al., 2012). An analytical form of the conventional horizontal weighting function has never been published. However, it can be derived from the cumulative function $\text{CFoC}(r)$, presented by Bogena et al. (2013, eq. 13), who fitted data from Zreda et al.

15   (2008, Fig. 3) in the domain of $r \leq 300\,\text{m}$:

$$
\begin{aligned}
e^{-r/127} \approx W^{\text{conv}}_{r \leq 300} &= \partial_r \text{CFoC}(r) \propto 1 - a_1 r + a_2 r^2 - a_3 r^3 + a_4 r^4 \\
\text{where} \quad a_i &= \left\{ 1.311 \cdot 10^{-2}, 9.423 \cdot 10^{-5}, 3.2 \cdot 10^{-7}, 3.95 \cdot 10^{-10} \right\}
\end{aligned}
\tag{4}
$$

   To account for the remaining contribution beyond $300\,\text{m}$, the (usually few) data points have been assigned the weight $W^{\text{conv}}_{r>300} = W^{\text{conv}}_{r=300}$. One of the major shortcomings of this exponential approach is the underestimation of the high sensitivity of the neutron signal to the first few meters around the sensor.

20   As a third strategy, we use the *revised* weighting approach based on URANOS simulations and corresponding analytical fits (see Köhli et al., 2015, for details). New technical advancements of this function include the dependency on air pressure p and humidity h by introducing the rescaled distance r^*, as well as the extension below $r \leq 0.5$ m.

$$
W_r(h, \theta, p, H_{\text{veg}}) =
\begin{cases}
\left(F_1 e^{-F_2 r^*} + F_3 e^{-F_4 r^*} \right) \left(1 - e^{-F_0 r^*} \right), & 0\,\text{m} < r \leq 1\,\text{m} \\
F_1 e^{-F_2 r^*} + F_3 e^{-F_4 r^*}, & 1\,\text{m} < r \leq 50\,\text{m} \\
F_5 e^{-F_6 r^*} + F_7 e^{-F_8 r^*}, & 50\,\text{m} < r < 600\,\text{m}
\end{cases}
\tag{5}
$$

   Parameter functions F_i, their corresponding parameters, the formulation of the rescaled distance $r^*(r, p, H_{\text{veg}}, \theta)$, as well as

25   further explanations are given in Appendix A.
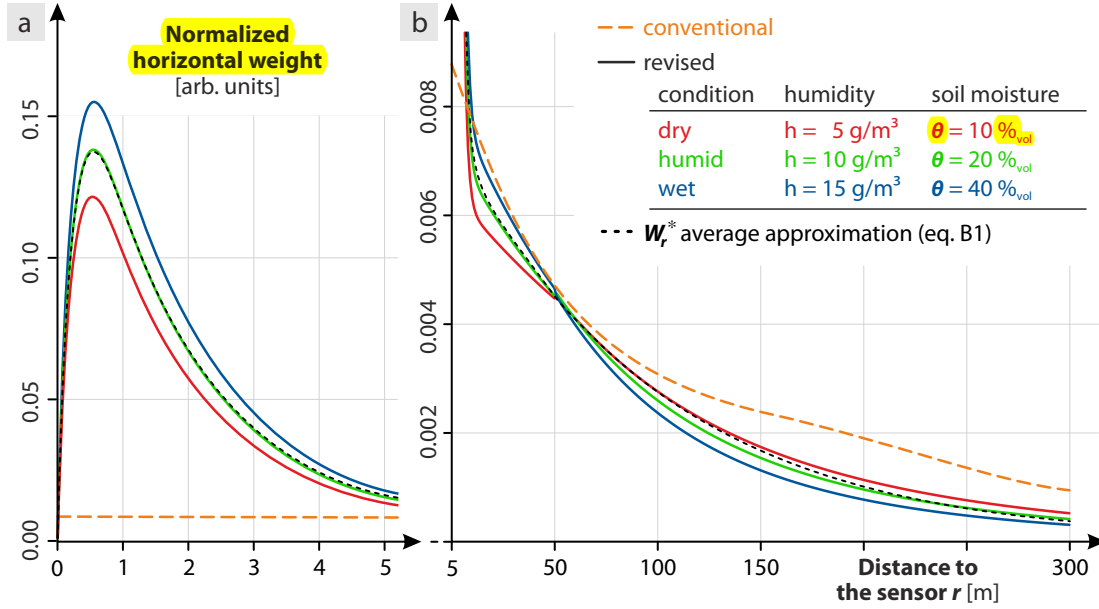
Figure 2. Comparison of normalized horizontal weighting functions (a) from 0 to 5 m, and (b) from 5 to 300 m. Graphs show the conventional (almost exponential) approach W_r^{conv} (eq. 4), the revised curves $W_r(h, \theta)$ for three wetness conditions (eq. 5), and an approximation W_r^* based on a simplified equation Appendix B. The *conventional* approach is insensitive to air and soil water content and highly underestimates the contribution of nearby areas ($r < 10$ m).

2.3 The Weighting Procedure

For each experimental site, consider a number of soil profiles P at distances r_P from the CRNS probe. In each profile, point measurements of volumetric water equivalent $\theta_{P,L}$ are given at various layers L of depth d_L. Observations of air pressure p, air humidity h, and vegetation height H_{veg} are given at the time of interest, while estimations of soil bulk density ϱ_{bulk} exist for

5 every profile (or even every sample). The general function to calculate an average of point measurements i with values θ_i and weights w_i is given as:

$$\text{wt}(\theta, w) = \frac{\sum_i w_i \theta_i}{\sum_i w_i}.$$

The procedure to obtain a weighted average of soil water equivalent, $\langle \theta \rangle$, is described as follows:

1. Estimate an initial value $\langle \theta \rangle = \text{wt}(\theta_{P,L}, 1)$ by an equally weighted average over all profiles P and layers L.

10 2. Calculate the penetration depth D_P for each profile P:

$$D_P^{\text{conv}} = z^*(\langle \theta \rangle),$$

or $D_P = D_{86}(\langle \theta \rangle, r_P^*).$

3. Vertically average the values $\theta_{P,L}$ over layers L, to obtain a weighted average for each profile P:

$$\theta_P^{\text{conv}} = \text{wt}\left(\theta_{P,L}, W_{d_L}^{\text{conv}}\right),$$

$$\text{or} \quad \theta_P = \text{wt}\left(\theta_{P,L}, W_{d_L}\right).$$

4. Horizontally average the profiles θ_P:

$$\langle\theta\rangle^{\text{conv}} = \text{wt}\left(\theta_P^{\text{conv}}, W_{r_P}^{\text{conv}}\right),$$

$$\text{or} \quad \langle\theta\rangle = \text{wt}\left(\theta_P, W_{r_P}\left(h, \langle\theta\rangle, p, H_{\text{veg}}\right)\right).$$

5. Use the new $\langle\theta\rangle$ to reiterate through steps 1.–5. until values converge.

The final averaged water equivalent $\langle\theta\rangle$ is then compared with the CRNS product, $\theta(N)$, derived from the neutron count rate N (eq. 1). It is also possible to calculate gravimetric water content using local bulk densities before step 3, however, URANOS calculations of W_r and W_d have been conducted only for homogeneous soil and volumetric water content (Köhli et al., 2015). While it has been assumed that N_0 accounts for persistent, non-homogeneous features in the footprint (Zreda et al., 2012), the influence of this state-of-the-art model assumption is to be investigated in future studies.

The above procedure weights each data point $\theta_{P,L}$ according to its depth d and distance r from the CRNS probe. However, when a finite number of sample points are chosen, assumptions are involved in the spatial domain they represent. Depending on knowlegde about the individual field conditions, interpolation between soil layers, for instance, is a good option to assign each measurement to a certain soil horizon. Let $\Omega(r, \vartheta)$ [m^3] be the spatial domain of the footprint volume in polar coodinates, Ω_P [m^2] the horizontal representative area of the profile P, and Ω_L [m] the representative soil horizon of the measurement at layer L. As each measurement $\theta_{P,L}$ is representing the volume $\Omega_P \cdot \Omega_L$, its weighted contribution to the neutron signal should be integrated over this domain:

$$\text{Horizontal contribution of profile } P: \quad w_P = \int_{\Omega_P} W_{r_P} = \int_{\Omega_P(r)} \frac{1}{2\pi} \int_{\Omega_P(\vartheta)} W_r \cdot d\vartheta \, dr,$$

$$\text{Vertical contribution of layer } L: \quad w_L = \int_{\Omega_L} W_{d_L} = \int_{\Omega_L(d)} W_d \cdot dd,$$

For example, if soil samples were taken at two depths, 10 cm and 40 cm for instance, it could be reasonable to integrate their weights from $d = 0$ to 30 cm and from 30 to 50 cm, respectively. In the horizontal space it might be sometimes reasonable to integrate a single profile measurement over the whole area of similar soil and landuse type (as has been done in section 4.4). If sample locations were arranged in an interpolated, regular grid (see e.g., Fig. 9), then each pixel should be weighted individually as a point such that the integrals above can be simplified. For example in a polar grid with 6 sectors, each sector at distance r is to be weighted with $\int_{\text{sector}} W_r = W_r/2\pi r \cdot (r/6) = W_r/(6\pi)$. In a rectangular grid of grid size s, the number of pixels per ring, n, at distance r is $n(r, s) = r/s$, such that the weight for each pixel is to be $\int_{\text{pixel}} W_r = W_r/(2\pi r) \cdot (r/n) \propto W_r/r$.

This strategy, to take into account estimations of representative volumes, initially appears to be more realistic. However, the extrapolation of data points involves assumptions on the site-specific heterogeneity and thereby on the strategy of interpolation.

It further requires expert knowledge about the individual field conditions. During the preparation of this work, we found that the usage of weights for distinct measurement points provided fair approximations of the integrals, i.e. $W_{r_P} \approx w_P$ and $W_{d_L} \approx w_L$, and eventually resulted in almost similar averages, $\langle\theta\rangle$, throughout all cases investigated (not shown).

2.4 Uncertainty due to partial coverage

5 In addition to the considerations about the representative domain, the arrangement of the soil samples can play a crucial role for the CRNS evaluation performance. If the locations of the soil samples (or in-situ monitored soil profiles) do not cover the CRNS footprint representatively, the corresponding data would not be able to explain parts of the neutron signal. Many sites exhibit highly irregular configurations where the soil monitoring network covers only parts of the CRNS footprint. The corresponding uncertainty in the CRNS evaluation can be estimated as follows.

10 Let S be the domain of the representative volume of the sample locations (e.g., the areal extent of the soil moisture monitoring network), and let Ω be the spatial domain of the CRNS footprint as defined in the previous section. Then, the outer region $\Omega \setminus S$ denotes the part of the footprint domain which is not represented by the samples. The contribution of the "sample area" S to the neutron signal then is:

$$\text{contribution:} \quad N_S/N_\Omega = \int\limits_S W_r \Big/ \int\limits_\Omega W_r \,,$$

15 which can range from 0 to 100 % and depicts the fraction of detected neutrons which carry information from (i.e., had contact with) the sample area S. Assume that the observed soil moisture in S is on average $\langle\theta\rangle$, and that the soil moisture in the outer region, $\Omega \setminus S$, can be estimated as $\langle\theta\rangle \pm \Delta\theta$. The propagation of this error through $W_r(h,\theta)$ leads to an uncertainty ΔN of the total neutron signal N,

$$N \pm \Delta N = \int\limits_\Omega W_r \approx \int\limits_S W_r(h,\langle\theta\rangle) + \int\limits_{\Omega\setminus S} W_r(h,\langle\theta\rangle \pm \Delta\theta) \,,$$

20 and eventually adds uncertainty to the CRNS product, $\theta(N \pm \Delta N)$. In this manuscript, this estimation is applied exemplarily to the *Schäfertal* site (section 4.2) in order to quantify the errors introduced by non-ideal coverage.

2.5 Performance Measures

To evaluate the performance of time series and calibration data, we apply prominent measures used in environmental and hydrological research. The robustness of this approach is evaluated by applying different performance measures, which is a 25 common strategy to falsify new methodological approaches (see e.g., Glaser et al., 2016). Popular efficiency measures are the *Nash-Sutcliffe-Efficiency* (NSE) (Nash and Sutcliffe, 1970) and the more modern *Kling-Gupta-Efficiency* (KGE) (Gupta et al., 2009), while the *Root-Mean-Square-Error* (RMSE) and the *Pearson correlation* coefficient (ρ) are well-established standard

approaches.

$$\text{NSE} = 1 - \frac{\sum(A-B)^2}{\sum(B-\langle B \rangle)^2}$$

$$\text{KGE} = 1 - \left[\left(\rho(A,B)-1\right)^2 + \left(\frac{\sigma_A}{\sigma_B}-1\right)^2 + \left(\frac{\langle A \rangle}{\langle B \rangle}-1\right)^2\right]^{\frac{1}{2}}$$

$$\text{RMSE} = \left\langle (A-B)^2 \right\rangle^{\frac{1}{2}}$$

$$\rho = \frac{\left\langle (A-\langle A \rangle)(B-\langle B \rangle) \right\rangle}{\sigma_A \sigma_B}$$

where $A = \theta(N, N_0)$ denotes the water equivalent measured by the CRNS (N_0 needs to be calibrated), B denotes the actual field soil water equivalent, θ, measured by independent instruments, and $\langle x \rangle = \frac{1}{n}\sum_1^n x$ denotes the average (expected value)

5 of a set of data points x. In the ideal case of optimal agreement between the variables A and B, the measures would reach NSE $= 1$, KGE $= 1$, RMSE $= 0$, and $\rho = 1$.

NSE normalizes the mean squared error by the observed variance, where the mean observed variable $\langle B \rangle$ is used as a baseline. Following this approach, site-specific variations could translate to biased estimation of model skills among different sites. On the other hand, the KGE measure is a revised version of NSE that allows to analyze the relative importance of linear

10 correlation ρ, variability σ, and bias $\langle \cdot \rangle$ of simulated and observed variables (Gupta et al., 2009). RMSE is simply a measure of the differences between two time series but is prone to biased datasets and outliers. The correlation ρ is an accepted approach in experimental geophysics to identify similar or unknown effects (e.g., Fu et al., 2015) in two time series. However, if many factors could explain a single observation, only using the correlation measure may lead to false recognition of coincidental effects.

15 The KGE is the most appropriate performance measure for time series data as it combines three distinct measures to optimally account for absolute errors and anomalies (compare also Heidbüchel et al., 2016). In the following analysis, we have thus optimized the KGE value between the CRNS and the independent soil moisture data to find a single calibration parameter N_0 per site.

3 Study sites

20 In order to provide a robust falsification of a potential benefit when using the revised weighted-averaging approach, datasets of six distinct sites have been consulted that offer comparison of the CRNS with independent soil moisture data under various climatic conditions (Fig. 3).

The Sheepdrove Organic Farm in Lambourn (UK). The *Sheepdrove Organic Farm* is located at (51.528175, -1.467311, 190 m asl) in the Lambourn catchment in South England. This region is characterized by a temperate climate with yearly

25 average precipitation of 815 mm, evenly distributed over the year, and with a mean daily maximum temperature of 14°C. The CRNS probe is located at a grass stripe which exhibits unmanaged soil and vegetation cover. The surrounding field is grazed by sheep during several variable periods throughout the year. During periods of sheep grazing and after harvest the height of
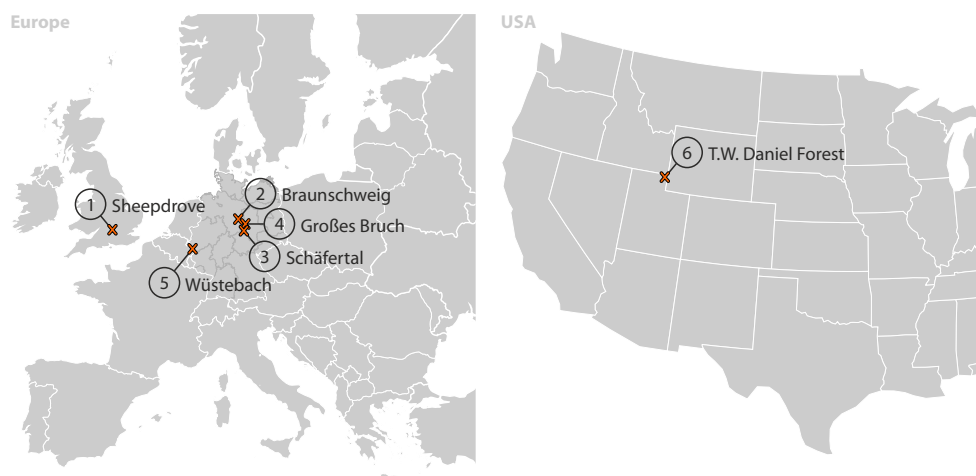
Figure 3. Selection of six distinct observation sites, five across Europe, and one in Utah/US.

the grass outside the strip is a few decimeters lower than within the strip. The soil is loamy clay with many flints and pieces of chalk. Weathered chalk starts at about 25 centimeters depth. The groundwater is tens of meters below the surface (Evans et al., 2016).

Agricultural site in the lowlands of Braunschweig (GER). The second calibration site is an irrigated agricultural field in
5   the northern lowland of Germany near Braunschweig, at an elevation of 60 m asl. Annual precipitation is 620 mm and average temperature 9.2°C. The 12 ha area is irrigated in 50 m wide strips with pre-treated waste water, as the sandy soils exhibit low water and nutrient holding capacity. The CRNS probe was located in the center of the field (52.3587°N, 10.4004°E) and several FDR devices provided point measurements of soil moisture. In 2014 the field was cropped with maize (Zea mays), that was drilled in mid-April harvested on September, 27th.

10   **The hillslopes and creek in the Schäfertal (GER).** The intensive monitoring site *Schäfertal* (11°03′ E, 51°39′ N, 395 m asl) is an agriculturally used catchment in the middle-mountain area of the Harz mountains in Central Germany (Zacharias et al., 2011; Wollschläger et al., 2016). Parts of the hillslope grassland transect is equipped with a wireless soil moisture monitoring network. It has a spatial extent of ca. 240 x 40 m and comprises a North- and a South-exposed slope as well as a valley bottom crossed by a creek oriented West to East. Silty-loam Cambisols occupy the slopes whilst finer-textured and highly organic soils
15   evolved in the riparian zone between the footslope and the creek (Martini et al., 2015).

The ponded flood plains at Grosses Bruch (GER). The research site *Grosses Bruch* is a mesophilic grassland used as meadow, within a nature protection area surrounding the water channel Grosser Graben (52.029728 N, 11.104678 E, 78 m asl) (Wollschläger et al., 2016). The grassland is usually flooded naturally once or twice a year. Soil type in the grassland is a sandy-loamy fluvisol-Gleysol, partly covered with a peat layer up to 1.5m depth. Eddy covariance measurements of energy, water,
20   carbon dioxide as well as methane are conducted at the site. Meteorological conditions as well as spatially distributed soil moisture and soil temperature in several depths are observed continuously with a wireless soil moisture monitoring network.

The forested Wüstebach catchment (GER). The Wüstebach test site is located in the German low mountain ranges within the borders of the Eifel National Park (50°30′ N, 6°19′ E) and is part of the TERENO Eifel/Lower Rhine Valley Observatory (Zacharias et al., 2011). The Wüstebach catchment covers an area of ≈ 38.5 ha with altitudes ranging from 595 m asl. in the northern part to 628 m asl. in the southern part. The soil types can be subdivided into terrestrial soils (i.e. Cambisols, Planosols)

5   and semi-terrestrial soils (i.e. Gleysols, Histosols) in the riparian zone (Gottselig et al., 2017). The mean porosity of the soils varied from 20 to $81\%_v$ for groundwater influenced soils and from 60 to $78\%_v$ for the terrestrial soils with decreasing values with increasing depth (Wiekenkamp et al., 2016). In the riparian zone, the water table varied between 0.0 and 1.6 m, while it constantly remained below the soil bedrock interface outside of the riparian zone (Bogena et al., 2015). The mean annual precipitation was 1220 mm between 1979 and 1999 and the mean monthly temperature varied from -1.5 to 15°C (Bogena

10 et al., 2010). Norway Spruce planted in 1946 is the prevailing vegetation type (Etmann, 2009; Baatz et al., 2014).

Complex landuse in the T.W. Daniel Experimental Forest (US). The T.W. Daniel Experimental Forest lies in one of mountaintops in the Wasatch Mountains (IMW), which is one of four components of Intermountain West of the United States and a transition zone of different climate regimes in both the seasonal and inter-annual time scales. The landscape of the TWDEF site is a patchwork of four domain vegetation communities common to the IMW. Forest communities include aspen

15 and conifer, predominantly Engelmann Spruce, and subalpine fir. Non-forest communities include grasses, forbs and sagebrush. For each dominant vegetation type, three plots and three subplots within each plot were randomly chosen, and TDT sensors were installed at 10 cm, 25 cm and 50 cm depth in each subplot (Lv et al., 2014).

General note: The experimental data collected in these sites can be classified with the following terminology. *Calibration datasets* typically denote soil samples taken at a single point in time, which are then analyzed for soil water content in the lab

20 and used to find a calibration parameter N_0 for the specific site. Notwithstanding, by repeating the sampling on other days also a validation can be addressed to some extent. *Validation datasets* typically denote time series measurements of a soil moisture monitoring network (SoilNet, Bogena et al. (2010)). They are used to validate the performance of the CRNS sensor, but can be also used to find the calibration parameter N_0 with the help of so-called performance measures. In the present work, we are using the terms *calibration site* and *validation site* only to distinguish between temporally distinct samples and continuous

25 data of independent soil moisture measurements, although in both cases those datasets are used to calibrate the CRNS probe.

4   Results and Discussion

The *equal*, *conventional*, and *revised* weighting approaches have been tested at six distinct research sites. In section 4.1 we have analyzed the calibration datasets at the *Sheepdrove Organic Farm* and at the *Braunschweig* site, in order to test the explanatory power of the theoretical relation, $N(\theta)$ (eq. 1). Section 4.2 discusses the uncertainty related to a time series dataset in the

30 *Schäfertal* catchment, where the footprint is only partly covered by monitored profiles. Section 4.3 analyzes the potential of CRNS and validation datasets in *Grosses Bruch* and *Wüstebach* to identify additional hydrological processes. At the *TWDEF* site in section 4.4, we use monitoring profiles in distinct parts of the footprint, which are individually weighted based on their areal contribution to the neutron signal.
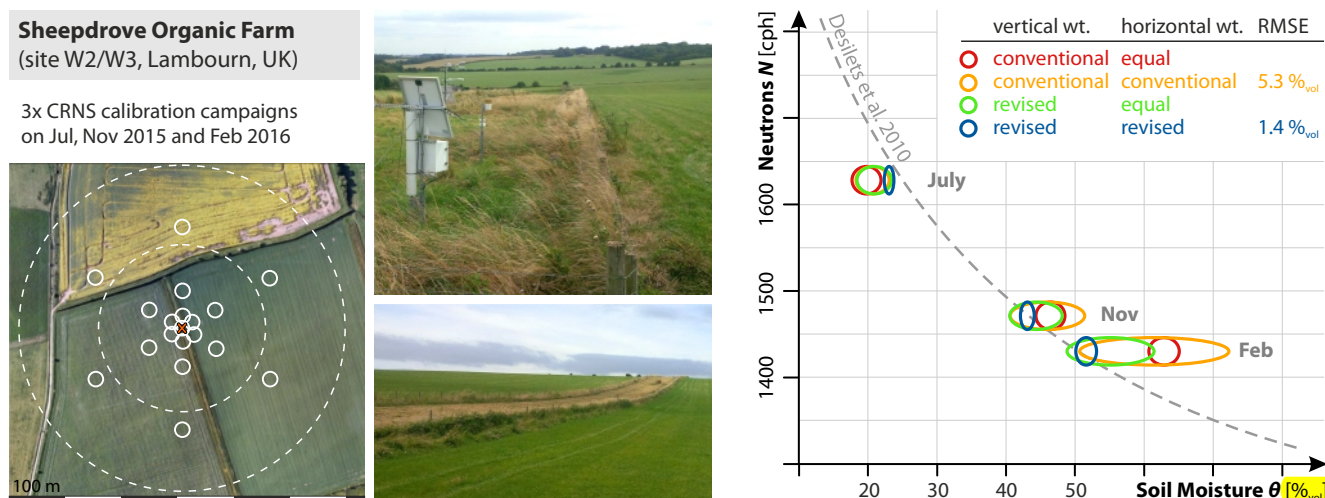
Figure 4. Recalibration of the CRNS sensor in the *Sheepdrove Organic Farm* (Lambourn, UK) using different combinations of vertically and horizontally weighted averages. Sizes of the circles indicate the corresponding uncertainty range of the measurement. The revised approach clearly removes the bias by the exceptional stripe around the sensor, improving the calibration performance with regards to the widely accepted theoretical relation (dashed).

4.1 Improvement of the calibration performance

In the farmlands of Great Britain, managed fields are often divided by stripes of hedges or unmanaged grassland. While unmanaged patches appear to be ideal positions for environmental-monitoring equipment, the presented example shows that CRNS measurements can be biased from the intended information about the field site. Three calibration datasets were collected at various wetness conditions within 9 months. The sampling design was based on the *COSMOS standard sampling scheme* at 25, 75, and 200 m, plus an additional location at 1 m near the CRNS probe. Fig. 4 demonstrates how the *equal* (red) and *conventional* (orange) weighting of the three calibration datasets deviate significantly from the single theoretical relation $N(\theta)$ (Desilets et al., 2010). By choosing the *revised vertical* weighting approach (green), the calibration points become much better in line with each other and reveal a single site-specific calibration curve. One of the reasons is the fact that the conventional approach neglects important parts of the sub-soil layers (beyond z^*), as indicated in Fig. 1b. Additional *revised horizontal* weighting (blue) leads to a precise match with the theoretical line, supporting the hypothesis that the samples within the stripe are most important to the CRNS signal. As a consequence of the difference between the soil moisture of the grass stripe and the surrounding agricultural fields (wetter in summer and dryer in winter), the application of a non-weighted calibration leads to significant over- or underestimation of the CRNS-apparent soil moisture value, respectively. Furthermore, the experiment clearly shows the importance of a proper positioning of the CRNS probe.

Insights from the British grassland have also been confirmed with calibration datasets from an ~~the~~ agricultural site near *Braunschweig*. Scheiffele (2015) used the *COSMOS standard sampling scheme* for three calibration campaigns during the
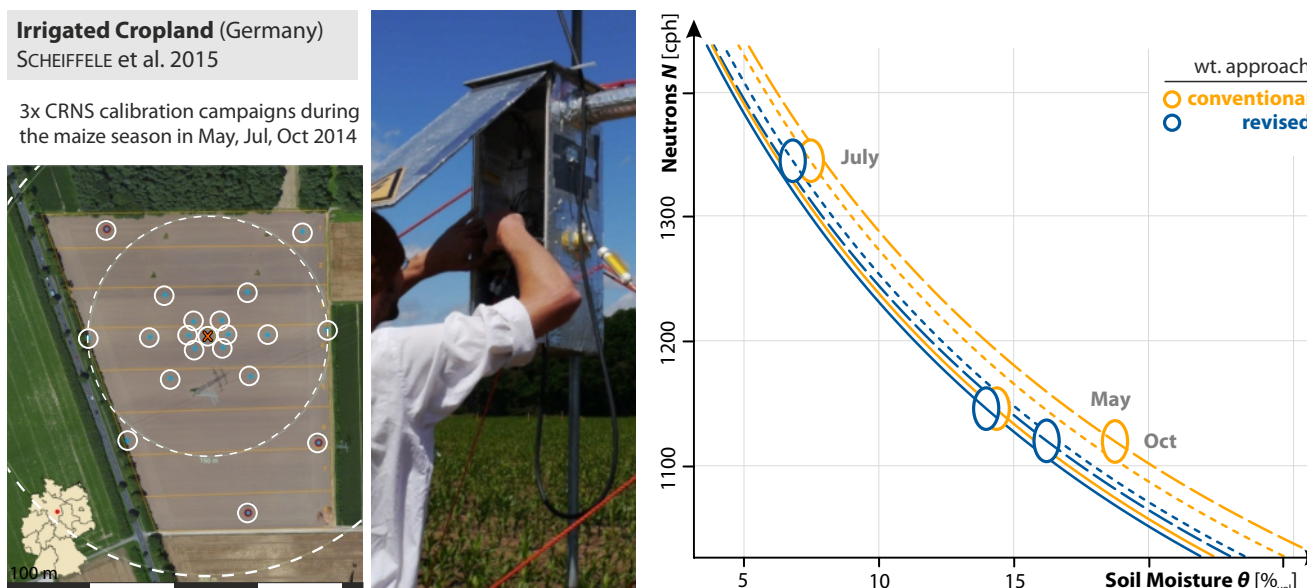
Figure 5. Recalibration of the CRNS sensor in an agricultural maize field (Braunschweig, Germany). Sizes of the circles indicate the corresponding uncertainty range of the measurement. The *conventional* weighting approach is not able to provide a single theoretical line through the three calibration days and further predicts unrealistic reduction of hydrogen pools during maximum plant height (July) and after harvest (Oct). The revised approach converges the datasets to confirm the accepted neutron theory almost in a single calibration curve.

agricultural season 2014 in May (no crop), July (maximum water content in biomass), and October (after harvest). Using the *conventional* averaging approach (orange), the calibration data in Fig. 5 could be interpreted as showing a reduced amount of hydrogen pools in the CRNS signal during the period of growing maize. This effect seems to be even higher in October than in July. This is opposed to observations by Franz et al. (2013b) and Baroni and Oswald (2015) who confirmed that the water

5 contained in crop biomass and below-ground residues typically adds to the apparent soil water equivalent.

  The data weighted with the *revised* functions demonstrates that the lines infered from the calibration points converge much closer to a single theoretical line (Desilets et al., 2010). Although this approach almost removes the unrealistic effect of reduced hydrogen pools, the assumption of a single calibration paramter N_0 must be considered to be illegitimate due to significant biomass dynamics in the investigated period. The remaining deviation of the three calibration curves still indicates a small

10 water reduction effect, however its magnitude is insignificant given the observational uncertainty of the neutron counter. It remains an open questions whether a revision of the parameters of eq. 1 would better catch the local dynamics and further contribute to the interpretation of the signal. Nevertheless, the example shows that the revised weighting strategy contributes to a more realistic interpretation of the water availability from CRNS measurements, which is especially important when used in conjunction with irrigation management.
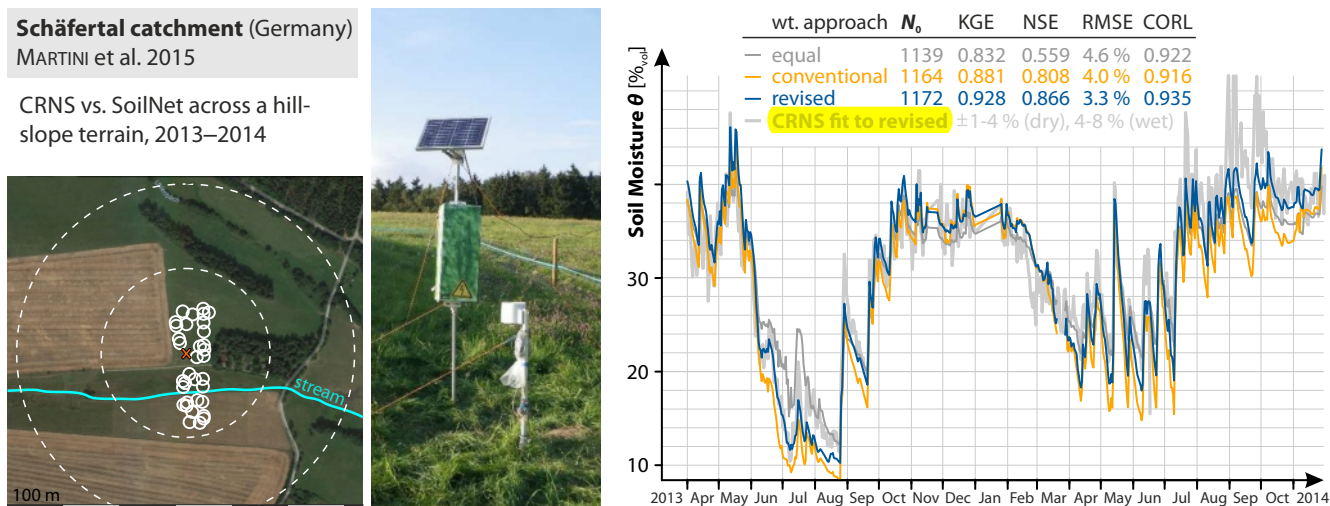
Figure 6. Time series of the CRNS soil moisture data at the SoilNet validation site in *Schäfertal* (Harz mountains, Germany). The *revised weighting approach improves four performance measures*, although the SoilNet probes are unevenly distributed in the CRNS footprint. The uncertainty introduced by the insufficient coverage ranges from 1 to $8\,\%_{vol}$ depending on wetness conditions.

4.2 Uncertainty estimation in a partly covered footprint

In the intensive monitoring site *Schäfertal* a CRNS probe is located in the center of a small area that is covered by the a soil moisture monitoring network. The CRNS footprint extends largely beyond this area, and rather involves patches of agricultural land and a nearby forest (Fig. 6). According to the guideline presented in section 2.4 the contribution of the SoilNet area
5   to the neutron signal ranges from 49% (dry) to 64% (wet). As a consequence, 36–51 % of the neutron variability cannot be explained by the irregularly distributed network. As an example case, one could assume an absolute variation of the outer area by $\Delta\theta = \pm 5\,\%_v$. Then the uncertainty of the CRNS soil moisture prediction can be further estimated following section 2.4. Under dry conditions ($\langle\theta\rangle \approx 15\,\%_v$), the propagated error is $\Delta\theta(N) \approx 1\text{–}4\,\%_v$, while under wet conditions ($\langle\theta\rangle \approx 35\,\%_v$) the neutron counts are less sensitive to soil moisture changes in the outer area due to the smaller footprint (Köhli et al., 2015). This
10   leads to $\Delta\theta(N) \approx 4\text{–}8\,\%_v$. Therefore, calibration results that resulted in an RMSE of $\approx 4\,\%_v$ (Fig. 6) are not meaningful under wet conditions (where $\Delta\theta(N) \geq 4\,\%_v$), and are still uncertain under dry conditions (where $\Delta\theta(N) \leq 4\,\%_v$). Consequently, the partial coverage of the CRNS footprint by the irregularly distributed SoilNet hampers the proper evaluation of the CRNS data, and especially of the weighting strategies.

Nevertheless, the *Schäfertal* data shows that the revised weighting approach is robust enough to improve the overall CRNS
15   performance (Fig. 6), even though the sensor is situated in complex terrain where the SoilNet sampling locations are not representative for the CRNS footprint. As the dominance of the revised approach in all four statistical measures is evident, the RMSE is still higher than the measurement error of the daily mean ($\approx 2\,\%_v$). This indicates that deviations can be attributed

(1) to the insufficient coverage of the SoilNet, and (2) to different processes in different parts of the footprint (e.g. vegetation growth, forest water interception, snow accumulation, evapotranspiration, plowing, etc.).

4.3 Identification of additional hydrological processes

The pasture site *Grosses Bruch* is a good example how an inappropriate averaging approach could hinder sufficient interpretation of time series data. Fig. 7 shows the soil moisture signal predicted from a stationary CRNS probe and the weighted signal of a soil moisture monitoring network (SoilNet) with sensors installed in depths from $0.05\,\mathrm{m}$ up to $0.6\,\mathrm{m}$. Following the precipitation events in the second half of October, the shallow groundwater and loamy texture allowed large water ponds to reside permanently in the outer regions of the SoilNet (light blue indication on the map). As distant areas contribute much less to the CRNS signal than closer ones, the *revised* weighting approach has significantly reduced the influence of the saturated point data to the apparent CRNS average. Without the revised method, the CRNS product would have overestimated the field saturation by more than $5\,\%_v$. Additionally, beginning in the mid of September a significant amount of cows were present at this site, which is assumed to lead to large variations of the neutron signal and thus to a non-meaningful expression of correlation-related measures.

In the *Wüstebach* forest site, weighted averaging of the soil moisture monitoring network is performed based on the data presented in Bogena et al. (2013). The analysis shows three interesting effects on the resulting soil moisture signal in Fig. 8. First, the signal processed with the *revised* weighting approach (blue) is wetter than the *conventionally* weighted signal (orange). This effect is reasonable due to the higher soil water contents of the groundwater-influenced riparian zone, where the CRNS is located, compared to the terrestrial soils at the hillslopes. Second, the CRNS signal which was calibrated to the *revised* weighted soil moisture (light blue) outperforms the signal that was calibrated on the *conventionally* weighted soil moisture (light orange). This performance gain is robust in terms of the four measures. In order to avoid conclusions from overcalibration of the data during rain events (periods of high interception water), we repeated the same analysis for dry periods only, which however resulted in the same conclusions (not shown). Third, differences between CRNS and SoilNet appear to be significantly more prominent for the *revised* approach (blue) in periods following huge precipitation events (May, July and October). Those periods can probably be attributed to expected canopy water storage, interception storage, groundwater rise, and nearby accumulation of ponds. Ponded water in local hollows, trenches, and the litter layer is not visible by the soil profiles of the monitoring network, which are typically installed in solid and elevated ground. In contrast, their effect can be visible in stronger oscillations and shift of the CRNS signal.

The analysis demonstrates that the *revised* weighting of calibration data is essential to identify residual hydrological effects which otherwise can get lost by overfitting. By comparing CRNS data and point measurements, residual information could be used to identify additional processes like biomass dynamics or rainfall interception (Baroni and Oswald, 2015). With the help of the methods presented here, we were able to identify those residuals to a much higher precision.
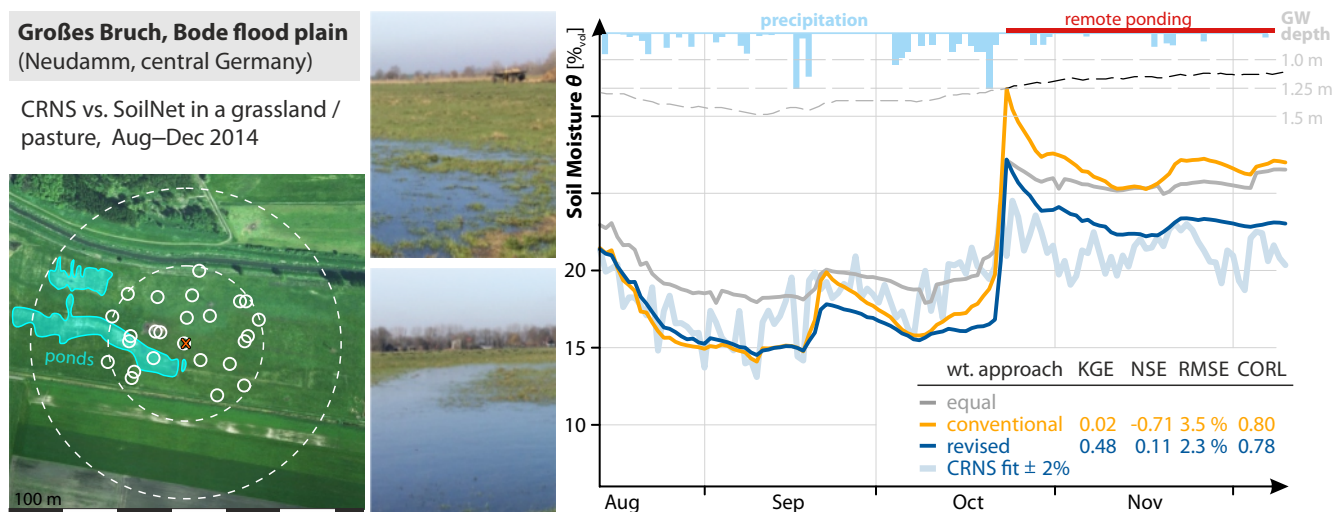
Figure 7. Time series of soil moisture measured in a pasture/floodplain *Grosses Bruch*. The rain events in mid-October 2014 lead to rise of the groundwater level and ponding in regions that are several tens of meters away from the neutron sensor. In that period, *equal* and *conventional* weighting leads to overestimation of apparent soil moisture near the CRNS probe, to which the detector has higher sensitivity than to the remote ponds.
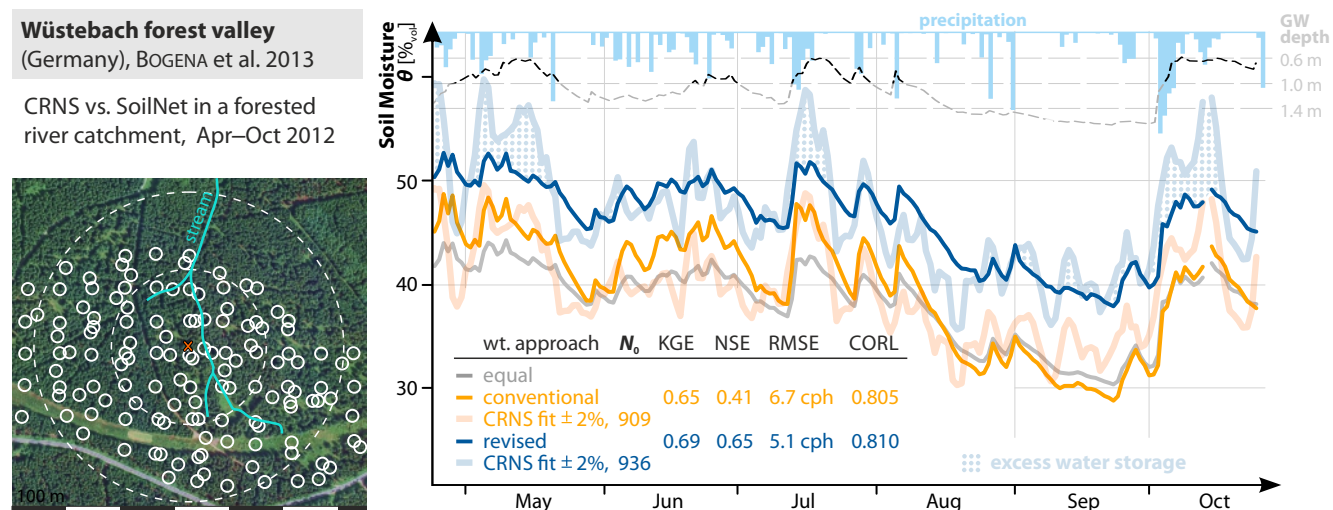
Figure 8. Time series of CRNS soil moisture and ground water at the forested river catchment *Wüstebach*. Fitting the CRNS data to the SoilNet *conventional* average almost completely hides effects like litter and interception water, groundwater rise, or ponding close to the stream. The *revised* approach emphasizes those additional hydrological processes, while still robustly increasing the sensor performance.
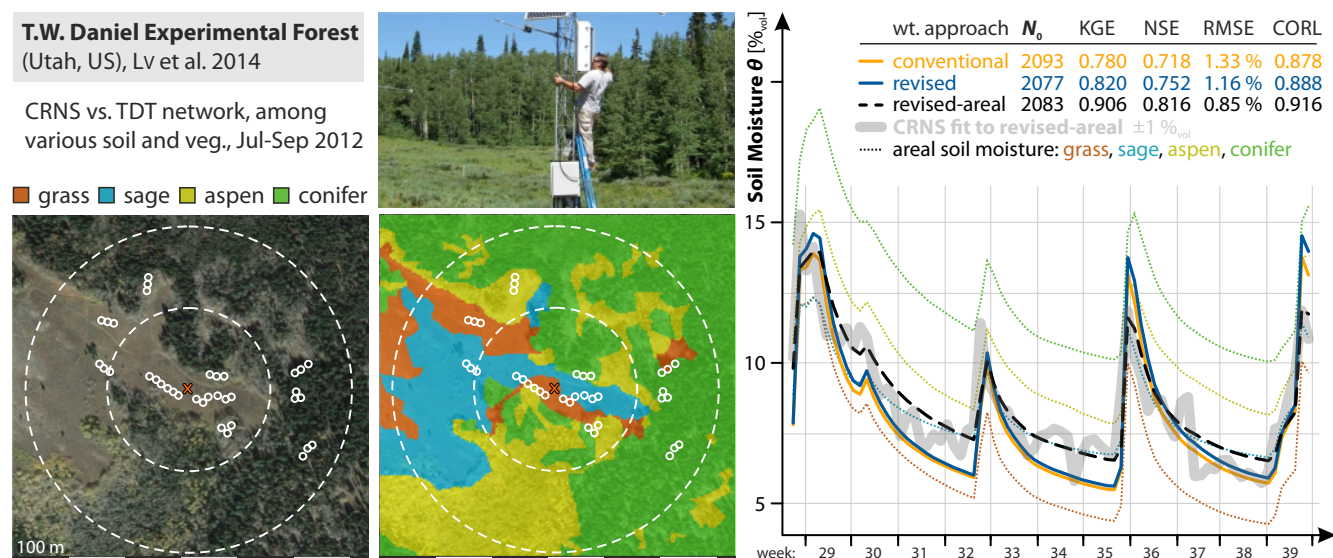
Figure 9. Time series of CRNS and TDT soil moisture at the *T.W. Daniel Experimental Forest*. The area was split into four categories (dotted lines), to which the corresponding soil moisture measurements were assigned. The areal coverage was then averaged (dashed line) with the revised weighting approach, leading to the best performance against the CRNS signal.

4.4 Areal contribution of distinct landuse classes

Lv et al. (2014) analyzed the CRNS performance in the centre of a complex mixture of grass and sage land, surrounded closely by an aspen and conifer forest located in the north of Utah/US. The authors took continuous TDT measurements in all four of those landuse types, complemented the dynamics of the soil moisture profiles with the help of HYDRUS-1D simulations, and found decent correlation to the CRNS signal (compare also similar approaches by Rivera Villarreyes et al. (2011) in a farmland). It is interesting to note that each of the four landuse compartments actually behaved very differently in terms of soil water dynamics, depicted as dotted lines in Fig. 9.

As each compartment is distributed differently in the CRNS footprint, the contribution of each area is different and thus cannot be averaged adequately by a simple weighting approach. However, in contrast to the complex terrain of the *Schäfertal* site (section 4.2), here all landuse and soil types are represented by adequate sample locations. We therefore grouped the soil moisture information of the four compartments, and weighted each $1\,\text{m}^2$ pixel of the areal contribution map depending on the pixel's distance r to the CRNS probe (see last paragraphs of section 2.3). This strategy again showed improved CRNS performance for all measures (black dashed line in Fig. 9) compared to the simple approach of weighting only the individual monitoring points (orange and blue, solid lines). Although the gained performance is not significant in the light of the measurement uncertainty, this areal weighting approach can be suggested as the most realistic representation of the contribution of heterogeneous soil moisture patterns to the CRNS signal.

Table 1. Descriptive summary of the various datasets analysed, using multiple calibration datasets, or time series data from soil moisture monitoring networks (e.g., SoilNet). At all sites, the robust approach either improves calibration/validation performance, or reveals hydrological processes that were otherwise hidden by over-calibration, or both.

dataset from	description	period	data type	gain
Sheepdrove Organic Farm, UK	grassland with central stripe	2015–2016	3 calib. days	data more consistent
Braunschweig, GER (Scheiffele, 2015)	irrigation agriculture	05–10/2014	3 calib. days	data more consistent
Schäfertal, GER (Martini et al., 2015)	heterogeneous hillslope	2012–2013	SoilNet	all measures improved
Grosses Bruch, GER	pasture grassland, floodplain	08–12/2012	SoilNet	revealed remote ponding
Wüstebach, GER (Bogena et al., 2013)	forested river catchment	04–08/2012	SoilNet	revealed additional hydrogen pools
T.W.D.E. Forest, US (Lv et al., 2014)	complex forest, grass, sage	2012–2013	TDT network	all measures improved (areal weight)

4.5 Summary of the analyzed research sites

The experimental sites used in this study and the corresponding gain for environmental and hydrological research is summarized in Table 1.

4.6 Towards a revised sampling scheme

5 The presented results are raising the question whether it could be profitable to apply a W_r-flavoured sampling design to the locations used for calibration and validation. Based on Zreda et al. (2008), the *conventional* weighting function W_r^{conv} laid the basis for the *COSMOS standard sampling scheme*, $R_i = \{25\,\text{m}, 75\,\text{m}, 200\,\text{m}\}$ (Franz et al., 2012a). These radii were located in the 33% quantiles of the footprint (see also Bogena et al., 2013, Table 3):

$$\frac{1}{3}\int_0^\infty W_r^{\text{conv}} \approx \int_0^{59} W_r^{\text{conv}} \approx \int_{59}^{186} W_r^{\text{conv}} \approx \int_{186}^\infty W_r^{\text{conv}}.$$

10 As Köhli et al. (2015) introduced the revised weighting function $W_r(h, \theta)$, the standard sampling scheme has become inappropriate, at least in non-homogeneous terrain, for two reasons: (1) the revised sensitivity is more steep, and (2) dynamically depends on wetness conditions. In particular, the dynamical horizontal weighting has been applied here to demonstrate its capability to significantly improve CRNS performance. While existing data from point sensor networks could be re-weighted in post-processing mode, the question arises whether positioning schemes for upcoming soil moisture networks or calibration

15 campaigns could adapt on the nature of neutron physics to maximize comparability.

Obviously, it is impossible to provide a new general position plan, due to the temporal variability of W_r and W_d, and the heterogeneity of local structures and conditions. Instead, selection of sampling locations should depend on (1) their representativeness for local features, and (2) their distance to the sensor. In general, it can be strongly recommended to select about half of available sampling points within the nearest $25\,\text{m}$, since the conventional sampling scheme from Franz et al. (2012a) does

20 not account for 40–50% of detected neutrons that originated in that area. To give further advice on a reasonable distribution of points for homogeneous terrain, sampling radii R_i of concentric circles could be calculated as follows.

First, select a total number of circles n based on prior knowledge about the patterns at the individual site. Since the signal contribution of an area between any radii can be calculated by integrating W_r (compare also Köhli et al., 2015, eq. 1), the n borders of equal areal contribution, r_i, $i \in (1, ..., n)$, can be calculated by solving the integral:

$$\int_0^{r_i} W_{r^*}(h, \theta) \, dr^* \overset{!}{=} \frac{i-1}{n} \int_0^\infty W_{r^*}(h, \theta) \, dr^* . \tag{6}$$

5   Then, the sampling radii R_i can be selected anywhere between r_i and r_{i+1}, as they are assumed to represent the area of the corresponding homogeneous annulus. A simple guideline could be to set the sampling radius in the geometrical center:

$$R_i(h, \theta, p, H_{\text{veg}}) = \begin{cases} r_i + 0.5 \, (r_{i+1} - r_i), & i < n, \\ r_i + 0.5 \, r_i, & i = n, \end{cases} \tag{7}$$

where the last sampling distance R_n could be set to any point that is expected to represent the whole area beyond r_n.

As an example for $n = 5$, Fig. 10a illustrates five annuluses of the footprint area which equally contribute to the neutron
10   signal. Therefore, an equal amount of sampling locations is recommended in each annulus. For example, using the hitherto common amount of 18 locations, we recommend for humid conditions to select 3 locations within $2\,\mathrm{m}$ distance, another 3 within $17\,\mathrm{m}$, and the remaining 3×4 locations distributed evenly within 58, 137, and $240\,\mathrm{m}$, respectively. In order to compare this approach with the conventional sampling scheme by Franz et al. (2012a), a 3-annulus scheme can be adapted from eq. 6 :

$$\text{dry:} \quad \frac{1}{3} \int_0^\infty W_{r^*} \approx \int_0^{24} W_{r^*} \approx \int_{24}^{108} W_{r^*} \approx \int_{108}^\infty W_{r^*} ,$$

$$\text{wet:} \quad \frac{1}{3} \int_0^\infty W_{r^*} \approx \int_0^{4} W_{r^*} \approx \int_{4}^{61} W_{r^*} \approx \int_{61}^\infty W_{r^*} .$$

15   Thus, if $n = 3$ radii are desired for the sampling scheme, a possible (but arbitrary) suggestion could be $R_i^{\text{dry}} \approx \{10\,\mathrm{m}, 65\,\mathrm{m}, 160\,\mathrm{m}\}$ and $R_i^{\text{wet}} \approx \{2\,\mathrm{m}, 25\,\mathrm{m}, 85\,\mathrm{m}\}$, as illustrated in Fig. 10b (compare also Heidbüchel et al., 2016, section 4.2).

This arrangement, however, should not relieve scientists of weighting their data in post-processing mode, because each annulus still exhibits a sensitivity gradient. But the $20\,\%$-annulus method strongly concentrates locations within most relevant regions favored by detectable neutrons. It is also worth noting that locations need not to be equally distributed among the
20   annuluses. The actual partitioning should rather be guided by expert knowledge about local correlation lengths of spatial soil moisture patterns. Given entirely homogeneous soil, for instance, a single location would do.

Having that said, is this strategy still robust against complex terrain and variable weather? Field sites differ in terms of spatial heterogeneity and variability due to terrain features or highly heterogeneous correlation lengths of soil moisture patterns. Hence, implementing a strict, universal sampling scheme often is neither feasible nor meaningful with regards to individual
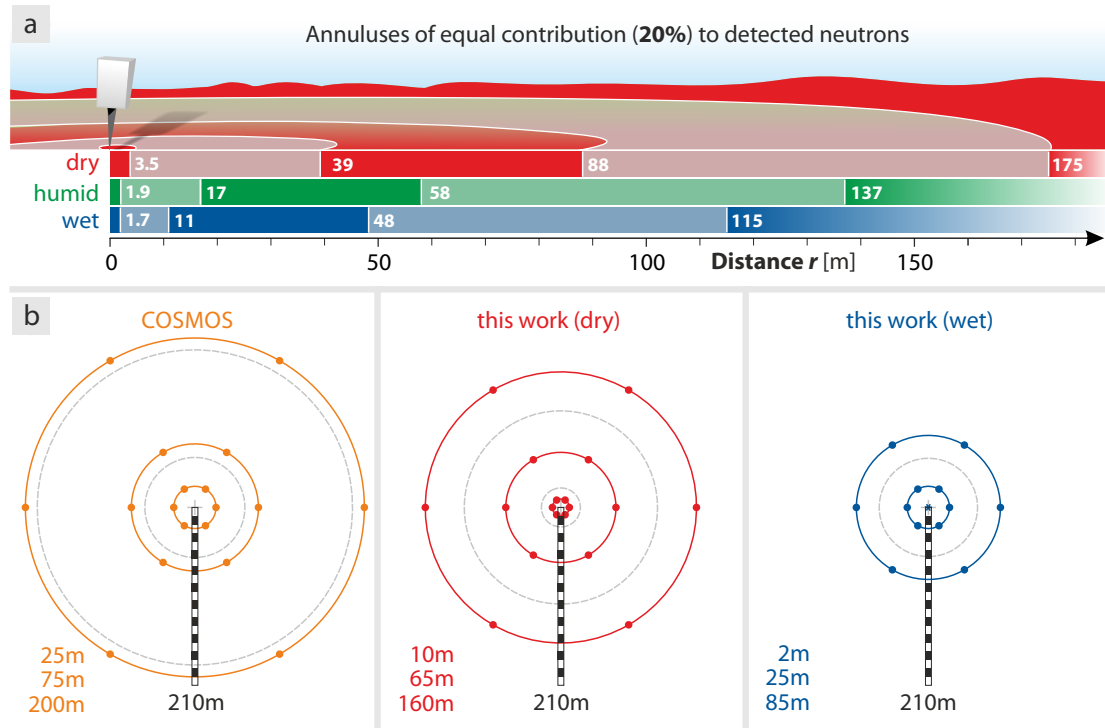
Figure 10. (a) Illustration of regions of equal contribution (20% quantiles) to the neutron signal for three climates, $h = \{2, 7, 20\}\,\mathrm{g/m^3}, \theta = \{2, 20, 50\}\,\%_v$. (b) The *COSMOS standard sampling scheme* based on W_r^{conv}, compared to two exemplary 3-radii-schemes based on the *revised* function W_{r*} for dry ($h = 1\,\mathrm{g/m^3}, \theta = 1\,\%_v$) and wet ($h = 10\,\mathrm{g/m^3}, \theta = 40\,\%_v$) conditions. Circles represent the borders of the 33% quantiles, r_i (grey, dashed), and arbitrary sampling distances R_i within these annuluses (colored, solid).

conditions in the field. In this study the application of the revised weighting approach led to improved CRNS performance at all sites and for regular and irregular sampling designs. Apparently, the presented weighting procedure is robust across various sites, sampling configurations, and wetness conditions.

An advantage of the approach is its straight-forward applicability, which essentially applies a simple distance-weighted

5   average to a set of data points, and does not require additional, complex analysis or interpolation strategies. The only assumption made is that each sample point represents an equal area in the footprint. Apart from sophisticated optimal sampling designs, three of the most simple sampling strategies are (1) regular grids, (2) random locations, and (3) locations that represent stable soil moisture patterns. However, judgment about their performance is far beyond the scope of this work. In any case, it could be recommended to reduce the uncertainty of locations close to the detector (e.g., by taking repeated measurements), because

10   neutron theory has shown that the CRNS signal is most sensitive to nearby locations.

In some cases it could help to choose sensor locations just in the way it is described by the approximated horizontal sensitivity function W_r^* (Appendix B). Under these conditions an equal average is sufficient in post-processing mode. However, the dependence on air humidity h and soil moisture θ will introduce temporal errors to this approach. In this case it could be

recommended to correct the equal average with its dynamic variability, which can be expressed as the variation of $W_r(h, \theta)$ around its mean, W_r^*.

To circumvent a potential bias introduced by arbitrarily distributed locations, it could be better to apply different zonation approaches or interpolation methods (e.g., Kriging in polar coordinates) before each cell of the interpolated grid is weighted.

5   However, this always comes with additional assumptions. For example, in the sampling strategy presented in section 4.4 certain soil moisture patterns in the field were categorized as four areas of different landuse which were expected to behave equally in the footprint in terms of soil water dynamics. The horizontal weighting was then applied to those measurements depending on the location of the contributing area in the footprint. In our opinion this method probably provides the highest accuracy in most cases, although it requires prior knowledge about the distribution of soil type compartments in the footprint.

10   This study has focused on the theory and application of the averaging approach, while the performance of different interpolation strategies might depend on local soil patterns and deserves a study on its own, for their performance always depend on the local structures and correlation lengths of soil moisture.

5   Conclusions

In this paper a general procedure for horizontal and vertical weighting of point measurements has been presented in order

15   to calibrate and validate the CRNS soil moisture product. The method is based on *revised* spatial sensitivity functions (or weighting functions) from neutron physics simulations (Köhli et al., 2015). Noteworthy, the *revised* functions have been further advanced in the present work with an updated version of the neutron transport code URANOS, by adding dependency on air pressure and vegetation height, and by extending the analysis to distances below $0.5\,\mathrm{m}$. The performance of the *conventional* weighting functions has been compared with the *revised* functions using datasets from a variety of distinct sites located in

20   Germany, the UK, and the US. The main conclusions are summarizes as follows:

1. The *revised* averaging of observed point data improved the performance measures when compared to the CRNS water equivalent, $\theta(N)$, for all investigated sites. The method is thus applicable to arbitrarily distributed sampling locations without prior knowledge of soil and landuse features.

2. The results show that unrealistic deviations of multiple calibration datasets from the theoretical line can be removed by

25   applying the revised weighting functions. Thus they support the original hypothesis by Desilets et al. (2010) of a single calibration campaign to capture the local soil moisture dynamics.

3. Although existing data can be weighted in post-processing mode, missing locations close to the detector as well as insufficient coverage of the CRNS footprint introduce significant uncertainty. It can be quantified with the help of the radial sensitivity functions, as has been presented section 2.4 and section 4.2.

30   4. Sampling strategies that are based on concentric rings can only be recommended for homogeneous terrain (where each sampling location is known to contribute equally to the signal) and should be adapted on the local site conditions (air

pressure, humidity, soil moisture, vegetation cover). If the samples are arranged according to eq. 7, their equally weighted average would provide a value that is comparable to the CRNS product. On the other hand, if the footprint is covered by heterogeneous soil and landuse patterns, the sample locations should be adapted to distinct representative clusters, which in turn should then be weighted based on their areal contribution to the signal (see section 4.4).

5. Data points in the first 0 to $10\,\mathrm{m}$ radius and 0 to $20\,\mathrm{cm}$ depth around the sensor are most important for calibration and validation purposes. It is thus recommended to reduce the uncertainty of those measurements, e.g., by avoiding flints in the samples, or by increasing the number of samples in that area.

6. As previous studies have shown, the CRNS soil moisture signal could be calibrated to match the simple, equal average of the areal soil moisture in the footprint. However, important hydrological features could be missed by doing so and data interpretation might become misleading. The revised weighting approach has the potential to reveal otherwise invisible hydrological features, like water in the biomass or litter layer, interception water storage, groundwater rise, as well as ponding in remote or local areas.

The revised weighting functions presented here are provided in the supplementary material in R, MATLAB, and Excel (see Appendix C). Furthermore, an approximated weighting function W_r^* (Appendix B) has been suggested to simplify quick analysis of the horizontal contributions independently of the local wetness conditions. However, the latter approach should be taken with care, for its adequate performance has not been sufficiently confirmed in this work.

Within this study many datasets have been reanalyzed to test the revised weighting approach. Due to its overall success, it is recommended to revisit also other studies, especially where the conventional approaches have not led to the expected results (e.g., Franz et al., 2012a; Almeida et al., 2014; Iwema et al., 2015). In the light of the discussion provided, we recommend future studies to improve the sensor performance even further. For example by investigating the effect of different sampling designs and interpolation strategies, or by recalibrating the parameters of the theoretical line, $N(\theta)$. Specific URANOS simulations of the neutron distribution at the individual sites can further help to identify the contribution to the detector signal of different parts in the footprint.

On the basis of the results gained by this study and in the light of the conclusions above, it can be deduced that CRNS stations placed in mostly homogeneous terrain offer the highest interpretability of its field-scale signal. This is a feature that the CRNS method has in common with many other hydrometeorologial instruments, like weather stations (Jarraud, 2008) or eddy covariance towers (Rebmann et al., 2005). However, even in complex terrain CRNS probes are capable to catch hydrogen pools that otherwise would be very difficult to monitor (e.g. ponding, interception), while their sensitivity to specific parts of the footprint can be quantified with the help of W_r. Thereby, the present study demonstrates a way forward to a better understanding of the spatial contributions to the neutron signal, and elaborates the potential of cosmic-ray neutron sensors to quantify hydrological features that are almost impossible to be caught with conventional instruments.

Appendix A: The revised weighting functions

Köhli et al. (2015) did not discuss in detail the dependencies of the weighting functions W_r and W_d on air pressure and humidity, although they made clear that these quantities have significant influence on the footprint radius. For this reason additional analysis has been performed to investigate the dependency of the sensitivity functions on other environmental variables, and

5 relations have been found that do not further complexify the analytical formulations of W_r and W_d. The weighting functions can easily adapt on variations of air pressure p and vegetation height H_{veg} by scaling their argument r with the scaling rules of the footprint radius R_{86} (cf. Köhli et al., 2015, eqs. 4–6):

$$W_r(h,\theta,p,H_{\text{veg}}) \approx W_{r^*}(h,\theta),$$

and $$W_d(\theta,r,p,H_{\text{veg}}) \approx W_d(\theta,r^*),$$ \qquad\qquad (A1)

where $$r^*(r,p,H_{\text{veg}},\theta) = r \cdot F_p \cdot F_{\text{veg}}(H_{\text{veg}},\theta).$$

Fig. 11 shows that this approximation performs well for various wetness conditions, as simulated curves and pressure-

10 adapted curves are almost parallel (relative agreement is sufficient as weighting functions typically perform in a relative mode).

Moreover, the data analysis in this work sometimes requires realistic weights to be applied for samples located within $r < 0.5\,\text{m}$, which is by definition an invalid range for $W_r(h,\theta)$ as reported by Köhli et al. (2015). We therefore felt the need to extend the horizontal weighting function to the range below $0.5\,\text{m}$. In this work, we introduced an additional exponential factor in eq. 5 which accounts for the steep increase near the detector. This peak has geometrical reasons and essentially comes from

15 the fact that (1) only few neutrons can originate from small radii ($W_{r\to 0} \to 0$), and (2) the neutrons coming from higher radii have a lower chance to hit the detector ($W_{r\to\infty} \to 0$).
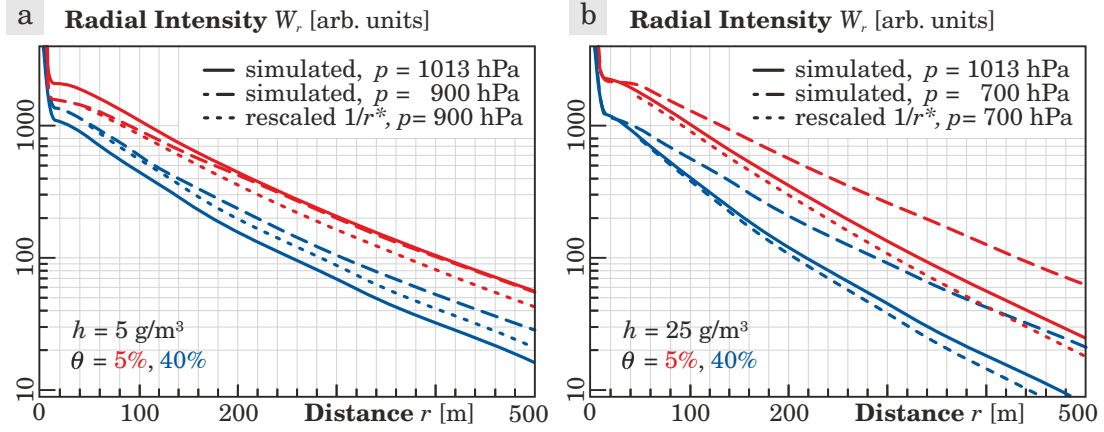
Figure 11. Pressure dependence of the weighting function W_r demonstrated for two cases of air pressure and humidity. The rescaled p-adapted curves (dots, eq. A1) are almost parallel to the non-adapted curves (solid), indicating that the normlized weight leads to the same results. (a) dry midlands, (b) humid highlands.

The following parameter functions apply to the updated weighting functions (cmp. also Köhli et al. (2015), Appendix A):

$$F_0 = p_0,$$

$$F_1 = p_0 (1 + p_3 h) e^{-p_1 \theta} + p_2 (1 + p_5 h) - p_4 \theta,$$

$$F_2 = \left((p_4 h - p_0) e^{-\frac{p_1 \theta}{1 + p_5 \theta}} + p_2 \right) (1 + p_3 h),$$

$$F_3 = p_0 (1 + p_3 h) e^{-p_1 \theta} + p_2 - p_4 \theta,$$

$$F_4 = p_0 e^{-p_1 \theta} + p_2 - p_3 \theta + p_4 h,$$

$$F_5 = \left(p_0 - \frac{p_1}{p_2 \theta + h - 0.13} \right) (p_3 - \theta) e^{-p_4 \theta} - p_5 h \theta + p_6,$$

$$F_6 = p_0 (h + p_1) + p_2 \theta,$$

$$F_7 = \left(p_0 (1 - p_6 h) e^{-p_1 \theta (1 - p_4 h)} + p_2 - p_5 \theta \right) (2 + p_3 h),$$

$$F_8 = \left((p_4 h - p_0) e^{\frac{-p_1 \theta}{1 + p_5 h + p_6 \theta}} + p_2 \right) (2 + p_3 h),$$

$$F_p = p_0 / \left(p_1 - e^{-p/1013 \, \mathrm{mbar}} \right), \quad \text{air pressure } p,$$

$$F_{\mathrm{veg}} = 1 - p_0 \left(1 - e^{-p_1 H_{\mathrm{veg}}} \right) \left(1 + e^{-p_2 \theta} \right), \quad \text{vegetation height } H_{\mathrm{veg}},$$

$$D_{86} = \frac{1}{\varrho_{\mathrm{bulk}}} \left(p_0 + p_1 \left(p_2 + e^{-p_3 r^*} \right) \frac{p_4 + \theta}{p_5 + \theta} \right), \quad \text{adapted distance } r^*.$$

Table 2. Parameters for the horizontal weighting function, the adapted distance scaling, and the effective penetration depth (Appendix A)

	p_0	p_1	p_2	p_3	p_4	p_5	p_6
F_0	3.7						
F_1	8735	22.689	11720	0.00978	9306	0.003632	
F_2	0.027925	6.6577	0.028544	0.002455	$6.851 \cdot 10^{-5}$	12.2755	
F_3	247970	23.289	374655	0.00191	258552		
F_4	0.054818	21.032	0.6373	0.0791	$5.425 \cdot 10^{-4}$		
F_5	39006	15002330	2009.24	0.01181	3.146	16.7417	3727
F_6	$6.031 \cdot 10^{-5}$	98.5	0.0013826				
F_7	11747	55.033	4521	0.01998	0.00604	3347.4	0.00475
F_8	0.01543	13.29	0.01807	0.0011	$8.81 \cdot 10^{-5}$	0.0405	26.74
F_p	0.4922	0.86					
F_veg	0.17	0.41	9.25				
D_{86}	8.321	0.14249	0.96655	0.01	20.0	0.0429	

Appendix B: A simplified approximation

As the analysis in this work has shown, the conventional horizontal weighting function can underrate soil moisture near the sensor by factors up to 25. Furthermore, the variability of the radial weighting function $W_r(h,\theta)$ with environmental conditions can have significant influence on the soil moisture average where accuracy matters. In cases where simplicity and computational

5   efficiency is a criterion, an *approximated weighting function W_r^** can be proposed, which is an averaged formulation over dry and wet conditions:

$$\langle W_r(h,\theta)\rangle_{h,\theta} \approx W_r^* = \begin{cases} \left(30\,e^{-r^*/1.6} + e^{-r^*/100}\right)\left(1 - e^{-3.7\,r^*}\right), & 0\,\mathrm{m} < r \leq 1\,\mathrm{m} \\ 30\,e^{-r^*/1.6} + e^{-r^*/100}, & r > 1\,\mathrm{m}. \end{cases} \tag{B1}$$

Fig. 2 shows the decent compromise performed by this approximation for both, short-range and long-range neutrons. Tests with all datasets of this study have indicated that the corresponding soil moisture average deviates from the exactly-weighted

10   average not more than $2\,\%_v$ (not shown). However, the deviation highly depends on h and θ and thus can be an important source of error in temporal analysis where large ranges of humidity are expected. Also note that the integral of the approximated function does not scale with neutron intensity anymore, which has however no impact on normalized weights.

Further studies will demonstrate whether eq. B1 is accurate enough to improve the CRNS performance under various wetness conditions and in different sites. If so, the reduction of computational effort will be valuable for regular analysis and for end

15   users in the applied sector.

Appendix C: Toolbox for spatial weighting of point data

Proper horizontal and vertical weighting of point measurements is a prerequisite for validation and calibration of the CRNS method. Before the publication of Köhli et al. (2015) almost all users of CRNS probes avoided horizontal weighting. However, the revised neutron physics model reveals a highly non-linear shape of the detector's radial sensitivity. The corresponding pub-

5 lication has been distributed with supplemental material that provided the weighting functions W_r as ready-to-apply `Excel`, `R` and `MATLAB` scripts. As the present study advanced the analytical fits of the spatial sensitivity functions (Appendix A), the corresponding updated script files can be found in the supplementary material.

Moreover, an easy-to-use toolbox has been prepared in form of an Excel sheet to guide users through the weighting process. This sheet is able to take a snapshot of point data around the sensor and calculates the corresponding CRNS footprint R_{86}, the

10 average penetration depth D_{86}, and the weighted average soil water content according to guidelines in this manuscript.

Acknowledgements. MS acknowledges kind support by the Helmholtz Impulse and Networking Fund through Helmholtz Interdisciplinary School for Environmental Research (HIGRADE). JI is funded by the Queen's School of Engineering, University of Bristol, EPSRC, grant code: EP/L504919/1. RR, JI and Sheepdrove Organic Farm activities are funded by the Natural Environment Research Council (A MUlti-scale Soil moistureEvapotranspiration Dynamics study (AMUSED); grant number NE/M003086/1). GB had financial support from the

15 Deutsche Forschungsgemeinschaft (DFG) under CI 26/13-1 in the framework of the research unit FOR 2131 "Data Assimilation for Improved Characterization of Fluxes across Compartmental Interfaces". CR and MC acknowledge the support of this study by the Integrated Carbon Observation System (ICOS) infrastructure through the Federal Ministry of Research and Education (BMBF). The research was funded and supported by the Terrestrial Environmental Observatories (TERENO), which is a joint collaboration program involving several Helmholtz Research Centers in Germany.

References

Almeida, A. C., Dutta, R., Franz, T. E., Terhorst, A., Smethurst, P. J., Baillie, C., and Worledge, D.: Combining Cosmic-Ray Neutron and Capacitance Sensors and Fuzzy Inference to Spatially Quantify Soil Moisture Distribution, IEEE Sensors Journal, 14, 3465–3472, doi:10.1109/JSEN.2014.2345376, 2014.

5 Baatz, R., Bogena, H., Franssen, H.-J. H., Huisman, J., Qu, W., Montzka, C., and Vereecken, H.: Calibration of a catchment scale cosmic-ray probe network: A comparison of three parameterization methods, Journal of Hydrology, 516, 231 – 244, doi:10.1016/j.jhydrol.2014.02.026, 2014.

Baroni, G. and Oswald, S.: A scaling approach for the assessment of biomass changes and rainfall interception using cosmic-ray neutron sensing, Journal of Hydrology, 525, 264–276, doi:10.1016/j.jhydrol.2015.03.053, 2015.

10 Bogena, H., Herbst, M., Huisman, J., Rosenbaum, U., Weuthen, A., and Vereecken, H.: Potential of wireless sensor networks for measuring soil water content variability, Vadose Zone Journal, 9, 1002–1013, 2010.

Bogena, H. R., Huisman, J. A., Baatz, R., Hendricks Franssen, H.-J., and Vereecken, H.: Accuracy of the cosmic-ray soil water content probe in humid forest ecosystems: The worst case scenario, Water Resources Research, 49, 5778–5791, doi:10.1002/wrcr.20463, 2013.

Bogena, H. R., Huisman, J. A., Güntner, A., Hübner, C., Kusche, J., Jonard, F., Vey, S., and Vereecken, H.: Emerging methods for noninvasive
15 sensing of soil moisture dynamics from field to catchment scale: a review, Wiley Interdisciplinary Reviews: Water, 2, 635–647, 2015.

Ceppi, A., Ravazzani, G., Corbari, C., Salerno, R., Meucci, S., and Mancini, M.: Real-time drought forecasting system for irrigation management, Hydrology and Earth System Sciences, 18, 3353–3366, doi:10.5194/hess-18-3353-2014, 2014.

Coopersmith, E. J., Cosh, M. H., and Daughtry, C. S.: Field-scale moisture estimates using COSMOS sensors: A validation study with temporary networks and Leaf-Area-Indices, Journal of Hydrology, 519, Part A, 637 – 643, doi:10.1016/j.jhydrol.2014.07.060, 2014.

20 Desilets, D. and Zreda, M.: Footprint diameter for a cosmic-ray soil moisture probe: Theory and Monte Carlo simulations, Water Resources Research, 49, 3566–3575, doi:10.1002/wrcr.20187, 2013.

Desilets, D., Zreda, M., and Ferré, T.: Nature's neutron probe: Land surface hydrology at an elusive scale with cosmic rays, Water Resources Research, 46, doi:10.1029/2009WR008726, 2010.

Etmann, M.: Dendrologische aufnahmen im wassereinzugsgebiet oberer wüstebach anhand verschiedener mess-und schätzverfahren, West-
25 fälische Wilhelms-Universität, Münster, Germany, 2009.

Evans, J., Ward, H., Blake, J., Hewitt, E., Morrison, R., Fry, M., Ball, L., Doughty, L., Libre, J., Hitt, O., et al.: Soil water content in southern England derived from a cosmic-ray soil moisture observing system–COSMOS-UK, Hydrological Processes, 30, 4987–4999, 2016.

Franz, T., Zreda, M., Rosolem, R., and Ferré, T.: Field Validation of a Cosmic-Ray Neutron Sensor Using a Distributed Sensor Network, Vadose Zone Journal, 11, doi:10.2136/vzj2012.0046, 2012a.

30 Franz, T., Zreda, M., Rosolem, R., Hornbuckle, B. K., Irvin, S. L., Adams, H., Kolb, T. E., Zweck, C., and Shuttleworth, W. J.: Ecosystem-scale measurements of biomass water using cosmic ray neutrons, Geophysical Research Letters, 40, doi:10.1002/grl.50791, 2013a.

Franz, T. E., Zreda, M., Ferré, T. P. A., Rosolem, R., Zweck, C., Stillman, S., Zeng, X., and Shuttleworth, W. J.: Measurement depth of the cosmic ray soil moisture probe affected by hydrogen from various sources, Water Resources Research, 48, doi:10.1029/2012WR011871, 2012b.

35 Franz, T. E., Zreda, M., Ferré, T. P. A., and Rosolem, R.: An assessment of the effect of horizontal soil moisture heterogeneity on the area-average measurement of cosmic-ray neutrons, Water Resources Research, 49, 6450–6458, doi:10.1002/wrcr.20530, 2013b.

Fu, C.-C., Wang, P.-K., Lee, L.-C., Lin, C.-H., Chang, W.-Y., Giuliani, G., and Ouzounov, D.: Temporal variation of gamma rays as a possible precursor of earthquake in the Longitudinal Valley of eastern Taiwan, Journal of Asian Earth Sciences, 114, Part 2, 362–372, doi:10.1016/j.jseaes.2015.04.035, earthquake Precursory Studies, 2015.

Glaser, B., Klaus, J., Frei, S., Frentress, J., Pfister, L., and Hopp, L.: On the value of surface saturated area dynamics mapped with thermal infrared imagery for modeling the hillslope-riparian-stream continuum, Water Resources Research, doi:10.1002/2015WR018414, 2016.

Gottselig, N., Wiekenkamp, I., Weihermüller, L., Brüggemann, N., Berns, A., Bogena, H., Borchard, N., Klumpp, E., Lücke, A., Missong, A., et al.: A Three-Dimensional View on Soil Biogeochemistry: A Dataset for a Forested Headwater Catchment, Journal of Environmental Quality, 46, 210–218, 2017.

Gupta, H. V., Kling, H., Yilmaz, K. K., and Martinez, G. F.: Decomposition of the mean squared error and NSE performance criteria: Implications for improving hydrological modelling, Journal of Hydrology, 377, 80–91, 2009.

Hawdon, A., McJannet, D., and Wallace, J.: Calibration and correction procedures for cosmic-ray neutron soil moisture probes located across Australia, Water Resources Research, 50, 5029–5043, doi:10.1002/2013WR015138, 2014.

Heidbüchel, I., Güntner, A., and Blume, T.: Use of cosmic-ray neutron sensors for soil moisture monitoring in forests, Hydrology and Earth System Sciences, 20, 1269–1288, doi:10.5194/hess-20-1269-2016, 2016.

Iwema, J., Rosolem, R., Baatz, R., Wagener, T., and Bogena, H. R.: Investigating temporal field sampling strategies for site-specific calibration of three soil moisture–neutron intensity parameterisation methods, Hydrology and Earth System Sciences, 19, 3203–3216, doi:10.5194/hess-19-3203-2015, 2015.

Jarraud, M.: Guide to meteorological instruments and methods of observation (WMO-No. 8), World Meteorological Organisation: Geneva, Switzerland, 2008.

Köhli, M., Schrön, M., Zreda, M., Schmidt, U., Dietrich, P., and Zacharias, S.: Footprint characteristics revised for field-scale soil moisture monitoring with cosmic-ray neutrons, Water Resources Research, 51, 5772–5790, doi:10.1002/2015WR017169, (M. Köhli and M. Schrön contributed equally to this work.), 2015.

Lv, L., Franz, T. E., Robinson, D. A., and Jones, S. B.: Measured and Modeled Soil Moisture Compared with Cosmic-Ray Neutron Probe Estimates in a Mixed Forest, Vadose Zone Journal, 13, –, 2014.

Martini, E., Wollschläger, U., Kögler, S., Behrens, T., Dietrich, P., Reinstorf, F., Schmidt, K., Weiler, M., Werban, U., and Zacharias, S.: Spatial and temporal dynamics of hillslope-scale soil moisture patterns: Characteristic states and transition mechanisms, Vadose Zone Journal, 14, 2015.

Nash, J. E. and Sutcliffe, J. V.: River flow forecasting through conceptual models part I—A discussion of principles, Journal of hydrology, 10, 282–290, 1970.

Norbiato, D., Borga, M., Degli Esposti, S., Gaume, E., and Anquetin, S.: Flash flood warning based on rainfall thresholds and soil moisture conditions: An assessment for gauged and ungauged basins, Journal of Hydrology, 362, 274–290, 2008.

Rebmann, C., Göckede, M., Foken, T., Aubinet, M., Aurela, M., Berbigier, P., Bernhofer, C., Buchmann, N., Carrara, A., Cescatti, A., et al.: Quality analysis applied on eddy covariance measurements at complex forest sites using footprint modelling, Theoretical and Applied Climatology, 80, 121–141, 2005.

Rivera Villarreyes, C. A., Baroni, G., and Oswald, S. E.: Integral quantification of seasonal soil moisture changes in farmland by cosmic-ray neutrons, Hydrology and Earth System Sciences, 15, 3843–3859, doi:10.5194/hess-15-3843-2011, 2011.

Robinson, D., Campbell, C., Hopmans, J., Hornbuckle, B., Jones, S. B., Knight, R., Ogden, F., Selker, J., and Wendroth, O.: Soil moisture measurement for ecological and hydrological watershed-scale observatories: A review, Vadose Zone Journal, 7, 358–389, 2008.

Samaniego, L., Kumar, R., and Zink, M.: Implications of Parameter Uncertainty on Soil Moisture Drought Analysis in Germany, J. Hydrom-eteor, 14, 47–68, doi:10.1175/jhm-d-12-075.1, 2013.

Scheiffele, L. M.: Assessment of soil moisture dynamics on an irrigated maize field using cosmic ray neutron sensing, Master's thesis, University of Potsdam, Institute of Earth and Environmental Science, Germany, 2015.

5 Schrön, M., Zacharias, S., Köhli, M., Weimar, J., and Dietrich, P.: Monitoring Environmental Water with Ground Albedo Neutrons and Cor-rection for Incoming Cosmic Rays with Neutron Monitor Data, in: 34th International Cosmic-Ray Conference (ICRC 2015), Proceedings of Science, http://pos.sissa.it/archive/conferences/236/231/ICRC2015_231.pdf, 2015.

Sheffield, J.: A simulated soil moisture based drought analysis for the United States, J. Geophys. Res., 109, doi:10.1029/2004jd005182, 2004.

10 Smith, M., Kivumbi, D., and Heng, L. K.: Use of the FAO CROPWAT model in deficit irrigation studies, FAO, Food and Agriculture Organization of the United Nations (FAO), 2002.

Vereecken, H., Huisman, J. A., Bogena, H., Vanderborght, J., Vrugt, J. A., and Hopmans, J. W.: On the value of soil moisture measurements in vadose zone hydrology: A review, Water Resources Research, 44, n/a–n/a, doi:10.1029/2008WR006829, 2008.

Wiekenkamp, I., Huisman, J., Bogena, H., Lin, H., and Vereecken, H.: Spatial and temporal occurrence of preferential flow in a forested
15 headwater catchment, Journal of hydrology, 534, 139–149, 2016.

Wollschläger, U., Attinger, S., Borchardt, D., Brauns, M., Cuntz, M., Dietrich, P., Fleckenstein, J. H., Friese, K., Friesen, J., Harpke, A., Hildebrandt, A., Jäckel, G., Kamjunke, N., Knöller, K., Kögler, S., Kolditz, O., Krieg, R., Kumar, R., Lausch, A., Liess, M., Marx, A., Merz, R., Mueller, C., Musolff, A., Norf, H., Oswald, S. E., Rebmann, C., Reinstorf, F., Rode, M., Rink, K., Rinke, K., Samaniego, L., Vieweg, M., Vogel, H.-J., Weitere, M., Werban, U., Zink, M., and Zacharias, S.: The Bode hydrological observatory: a platform for
20 integrated, interdisciplinary hydro-ecological research within the TERENO Harz/Central German Lowland Observatory, Environmental Earth Sciences, 76, 29, doi:10.1007/s12665-016-6327-5, 2016.

Zacharias, S., Bogena, H., Samaniego, L., Mauder, M., Fuß, R., Pütz, T., Frenzel, M., Schwank, M., Baessler, C., Butterbach-Bahl, K., et al.: A Network of Terrestrial Environmental Observatories in Germany, Vadose Zone Journal, 10, 955–973, doi:10.2136/vzj2010.0139, 2011.

Zink, M., Samaniego, L., Kumar, R., Thober, S., Mai, J., Schäfer, D., and Marx, A.: The German drought monitor, Environmental Research
25 Letters, 2016.

Zreda, M., Desilets, D., Ferré, T. P. A., and Scott, R. L.: Measuring soil moisture content non-invasively at intermediate spatial scale using cosmic-ray neutrons, Geophysical Research Letters, 35, doi:10.1029/2008GL035655, 2008.

Zreda, M., Shuttleworth, W. J., Zeng, X., Zweck, C., Desilets, D., Franz, T., and Rosolem, R.: COSMOS: The COsmic-ray Soil Moisture Observing System, Hydrology and Earth System Sciences, 16, 4079–4099, doi:10.5194/hess-16-4079-2012, 2012.